Size-Dependent Activity of Co₃O₄ Nanoparticle Anodes for Alkaline Water Electrolysis

Arthur J. Esswein, Meredith J. McMurdo, Phillip N. Ross, Alexis T. Bell,* and T. Don Tilley*

*Departments of Chemistry and Chemical Engineering, University of California, Berkeley,
Berkeley, California 94720, and the Chemical Sciences Division, Lawrence Berkeley National Laboratory,
1 Cyclotron Road, Berkeley, California 94720*

Cubic Co_3O_4 nanoparticles with average diameters of 5.9, 21.1, and 46.9 nm (hereafter small, medium, and large) have been synthesized and characterized by pXRD, TEM, and BET. The nanoparticles were loaded onto Ni foam supports for evaluation as anodes for water electrolysis in 1.0 M KOH. Current densities of 10 mA/cm² were achieved at overpotentials of 328, 363, and 382 mV for anodes loaded with 1 mg/cm² of small, medium, and large sized Co_3O_4 nanoparticles, respectively. The activity correlates with the BET surface area of the isolated particles. A plot of the electrochemical overpotential at 10 mA/cm² against the log of the BET surface area gives a linear relation with a slope of -47 ± 7 mV/dec, showing unequivocally that the activity increase is a function of accessible catalyst surface area.

Introduction

The dual concerns of energy security and climate change have stimulated considerable interest in renewable energy sources,[1,2] primarily in the form of electricity derived from solar photovoltaics and wind turbines. While abundant, solar and wind are intermittent power sources; their generation is not matched with the constancy of terrestrial energy utilization. Due to this variability, renewable energy cannot realistically contribute to our energy portfolio until these intermittent sources can be stored and distributed in a fashion commensurate with use. Thus, to match the supply of energy with demand, it is necessary to have means for storing energy. Storage solutions in the form of batteries, capacitors, and flywheels do not have the energy density and scalability required to meet projected energy demands, leaving only the conversion of renewable electricity to chemical fuels as a viable option.[3] Water splitting, to produce hydrogen and oxygen, has long been considered a desirable option for the storage of electrical energy. Powering modern society with nonfossil energy remains a grand challenge for both science and engineering, but efficient methods for the conversion of renewable-derived electricity into storable fuels represents a promising pathway toward this goal.

Interest in electrolytic routes to water splitting is longstanding,[4] with the bulk of the research effort concentrated on the more challenging anodic oxidation of water to oxygen. Prior work has shown that noble metals (e.g., Pt, Pt/Ru) and noble metal oxides (e.g., RuO_2 and IrO_2) are effective anode electrocatalysts exhibiting high activities and, hence, low overpotentials.[5] Over the past 30 years, significant research has focused on discovering base metal alternatives to these expensive noble metal electrode materials. A very large number of candidate materials have been examined, focused mostly on the oxides of Fe, Mn, Ni, and Co, including simple oxides such as Fe_3O_4, MnO_2, NiO, and Co_3O_4 and complex oxides such as $NiCo_2O_4$ in addition to other mixed metal spinels and perovskites.[5–8] Of these materials, particular attention has been given to the cobalt oxide spinel, Co_3O_4, which has been shown to be an effective

anode material for various oxidation reactions including $Cl^- \rightarrow Cl_2$,[9] $CO \rightarrow CO_2$,[10] $EtOH \rightarrow AcOH$,[11] and of pertinence to this report, $H_2O \rightarrow O_2$.[5–8,12–14] A truly ubiquitous redox catalyst, Co_3O_4 has also been investigated for oxygen reduction[15] and also as a Li intercalation material for the electron on/off charging cycles of Li ion batteries.[16] For electrocatalytic oxygen evolution, Co_3O_4 and other base metal oxides are typically used in concentrated base (1–8 M KOH) where the pertinent redox half reactions at the anode and cathode are described by eqs 1 and 2, respectively

$$4\,OH^- \rightarrow O_2 + 4\,e^- + 2\,H_2O \qquad (1)$$

$$4\,H_2O + 4\,e^- \rightarrow 2\,H_2 + 4\,OH^- \qquad (2)$$
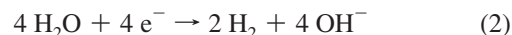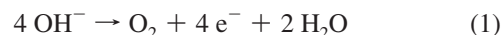
The utility of alkaline solution is two-fold: to inhibit metal or oxide corrosion by decreasing the requisite potential at the anode and to increase solution conductivity. Recently, however, a means for growing a cobalt oxide catalyst layer electrochemically in the presence of phosphate anion at neutral pH has also been described.[17]

In this report we aim to elucidate the size dependence of Co_3O_4 crystallites on electrocatalytic oxygen evolution activity in a well-defined manner. A simple hypothesis is that, in the absence of defect effects or edge effects, the larger the catalyst surface area, the greater the catalytic activity. Synthetic methods targeting nanometer-sized materials have advanced to the point where the desired material size or shape can be produced with ease. Thus, nanomaterials present an intriguing opportunity for defining size-activity relationships for a "dimensionally stable anode" material such as Co_3O_4.

Experimental Methods

Nanoparticulate Co_3O_4 was synthesized by a literature procedure.[18] In our hands the smallest particles obtained were slightly larger than those described in the literature report, but this discrepancy is likely due to the sensitivity of nanoparticle synthesis to specific reaction vessels and procedures. NH_4OH

---

* To whom correspondence should be addressed. E-mail: bell@cchem.berkeley.edu (A.T.B.); tdtilley@berkeley.edu (T.D.T.).

Size-Dependent Activity of Co$_3$O$_4$ Nanoparticle Anodes

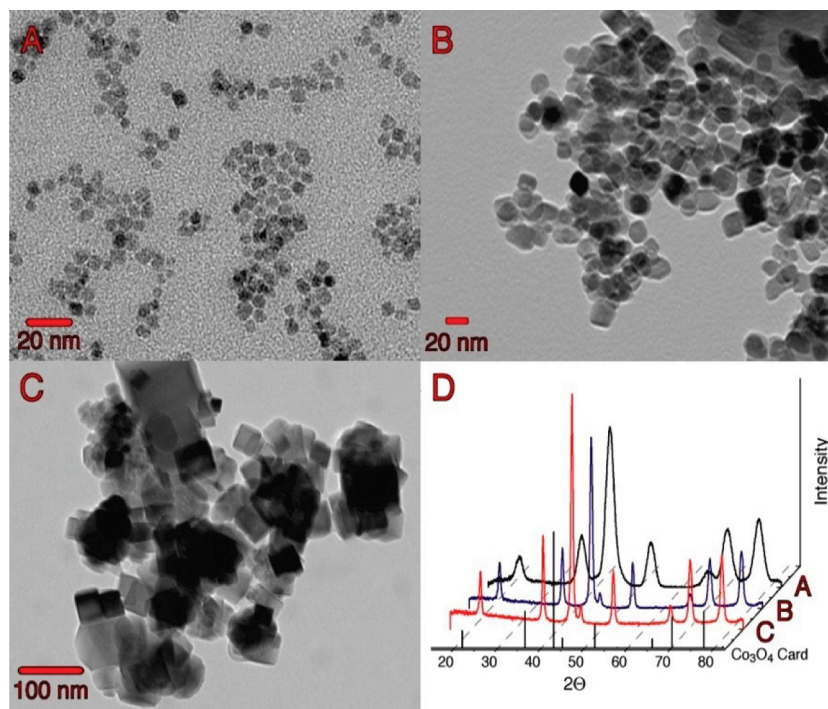*J. Phys. Chem. C, Vol. 113, No. 33, 2009* **15069**

Figure 1. TEM images of cubic nanoparticles of Co$_3$O$_4$ with average sizes of (A) 5.9 ± 1.0, (B) 21.1 ± 5.4, and (C) 46.9 ± 23.6 nm. (D) pXRD patterns for the particles from panels A−C with the Co$_3$O$_4$ card shown for reference.

(28−30%), KOH, EtOH (EMD), Co(OAc)$_2$·4(H$_2$O) (Alfa) were obtained from the suppliers indicated and used as received. Distilled water was used throughout. Labeled water, 95% ^{18}O (Cambridge Isotope Laboratories), was diluted with distilled water and KOH to give a final solution with 8.45% total ^{18}O content.

Transmission electron microscopy (TEM) was carried out on a Philips Tecnai 12 transmission electron microscope operating at 200 kV. Samples for TEM studies were prepared by depositing an aqueous suspension of the material onto a carbon-coated copper grid obtained from Ted Pella, Inc. Powder X-ray diffraction (pXRD) patterns were recorded on a Bruker D-8 GADDS X-ray diffractometer using Co Kα radiation (λ = 1.7902 Å), and were indexed to card 01-071-4921 (Co$_3$O$_4$) for reference. The College of Chemistry Microanalytical Laboratory at the University of California Berkeley performed carbon, hydrogen, and nitrogen elemental analysis; all nanoparticle samples returned CHN weight percents of zero within the error of the measurement. Nitrogen sorption isotherms were obtained using a Quantachrome Autosorb 1, and samples were outgassed at 120 °C for at least 15 h prior to measurement. pH measurements were conducted using a Thermo Orion 2 star pH meter. Electrochemical data were recorded on a Bioanalytical Systems model CW50 computer controlled potentiostat. Unless otherwise noted all measurements were performed in a two compartment H-cell using a standard three electrode configuration. Catalytic runs were collected in 1 M KOH (measured as pH 14.0) and referenced to a Ag/AgCl reference electrode. In this report the thermodynamic potential for the anode, $E^{\circ}_{OH^-/O_2}$ = 0.403 V vs NHE at pH 14 (0.206 V vs Ag/AgCl), was used for all overpotential measurements. A 1 cm × 1 cm piece of platinum mesh served as the auxiliary electrode. Working electrodes comprised of 1 cm × 1 cm × 0.1 cm pieces of nickel foam (Marketech International, Port Townsend WA) loaded with Co$_3$O$_4$ completed the standard three-electrode configuration. Well-defined loadings of Co$_3$O$_4$ on the Ni foam were achieved by suspending 10.0 mg of Co$_3$O$_4$ nanoparticles

in 10.0 mL of distilled water with sonication followed by deposition of a known volume of this solution on the Ni foam electrode, and final evaporation of the water with a heat gun on a low setting. Typical Co$_3$O$_4$ loadings of 1 mg/cm^2 (geometric anode area) were achieved in this manner. Oxygen isotope experiments were conducted using a single-compartment airtight cell equipped with a valve for periodic sampling of the reaction headspace. Prior to electrolysis the solutions were degassed with high purity argon for 20 min. The headspace gas was then fed through a high-vacuum line into a Pfeiffer Omnistar 422 quadrupole mass spectrometer for analysis. The resulting mass spectra were corrected for signals resulting from the argon carrier gas by first measuring a MS of the argon, then the electrolyzed samples and the argon background were normalized to the signal at m/z = 40 and finally the background argon spectrum was subtracted from that of the sample.

Results and Discussion

Cubic Co$_3$O$_4$ nanoparticles were prepared according to the method of Zhang and co-workers,[18] wherein solutions of hydrated cobalt acetate were treated with aqueous ammonium hydroxide and heated at 150 °C in an autoclave for 3 h. The nanoparticle size could be changed using this method by varying the water content in an ethanol/water solvent system. The attractiveness of this particular method is its simplicity and the absence of surfactants or other surface stabilization groups typically employed in nanoparticle synthesis. As a result, particles are produced that are free of organic matter, which might inhibit or poison their catalytic activity.

TEM images of the as-synthesized particles reveal cubic structures with average diameters of 5.9 ± 1.0, 21.1 ± 5.4, and 46.9 ± 23.6 nm (herein small, medium, and large, respectively; sizes are based on the average of 100 measured particles), and are shown in panels A, B, and C of Figure 1, respectively. As noted in Table 1, the dispersion of these particles increases with increasing particle size from 15% to 50%. pXRD patterns of

15070 *J. Phys. Chem. C, Vol. 113, No. 33, 2009*

Esswein et al.

TABLE 1: Physical Characterization Data for the As-Synthesized Co_3O_4 Nanoparticles

| TEM (nm)[a]	pXRD (nm)[b]	BET SA (m²/g)	calcd SA (m²/g)[c]
5.9 ± 1.1	10.1	111.2	157.7
21.1 ± 5.4	32.6	27.93	44.1
46.9 ± 23.6	34.2	7.80	19.8

[a] Mean size calculated from observation of 100 particles in the TEM images. [b] Calculated crystallite size from Debeye−Scherrer analysis of the (400) line in the pXRD patterns. [c] Calculated surface area assuming perfect cubes with side lengths dictated by the TEM results.

the particles show lines corresponding exclusively to cobalt oxide spinel (card 01-71-0816). The average particle size, assuming spherical particles, was determined by a Debeye−Scherrer analysis[19] of the (400) lines in each sample and gives values lying between 10.1 and 34.2 nm. The correlation between crystallite sizes calculated from pXRD data and those observed by TEM is generally good. Brunauer−Emmett−Teller (BET) measurements of the particle surface areas gave values of 111.2, 27.93, and 7.80 m²/g for the small, medium, and large particles, respectively. These experimentally observed values compare favorably with the surface areas of 157, 44, and 20 m²/g calculated by assuming perfect cubes of Co_3O_4 with edge lengths equated to the average diameters measured in the observed TEM images. The BET surface areas are systematically lower than those estimated from the average particle size due possibly to particle aggregation.

Cyclic voltamograms of Ni foam anodes deposited with the Co_3O_4 nanoparticles (by the method described in the experimental section) in 1.0 M KOH recorded at 50 mV/s in a two-compartment H-cell (Pt-mesh auxiliary electrode and an Ag/AgCl reference electrode) show a broad anodic wave at ~475 mV (Figure S1, Supporting Information) attributable to the adsorption and subsequent oxidation of hydroxide at an active surface site (S), eq 3.[20]

$$S + OH^- \rightarrow SOH + e^- \qquad (3)$$

Interestingly, the anodic wave attributed to the $Ni(OH)_2 \rightarrow Ni(O)(OH)$ redox couple, observed at ~375 mV on the bare Ni foam electrode, is absent from the voltammogram of all electrodes loaded with Co_3O_4 (Figure S1, Supporting Information). This suggests that the spinel nanoparticles effectively cover the Ni foam substrate and insulate the Ni substrate from solution-based redox chemistry at the anode surface, implying that a background correction for the Ni foam support is unnecessary for all Co_3O_4 coated anodes. Biasing the anode at more positive potentials results in a sharp increase in current commencing around 650 mV. At these potentials vigorous gas evolution is observed at both the anode and cathode suggestive of catalytic water electrolysis. The catalytic current has been attributed to a chain of redox events that begin with the oxidation of a surface hydroxyl to give a surface bound oxo, eq 4.

$$SOH + OH^- \rightarrow SO + e^- + H_2O \qquad (4)$$

$$2\,SO \rightarrow S + O_2 \qquad (5)$$
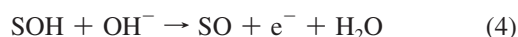
The catalytic cycle is then closed by the reaction of two surface oxos to generate oxygen and regenerate the active surface site (eq 5). It should be noted, though, that while
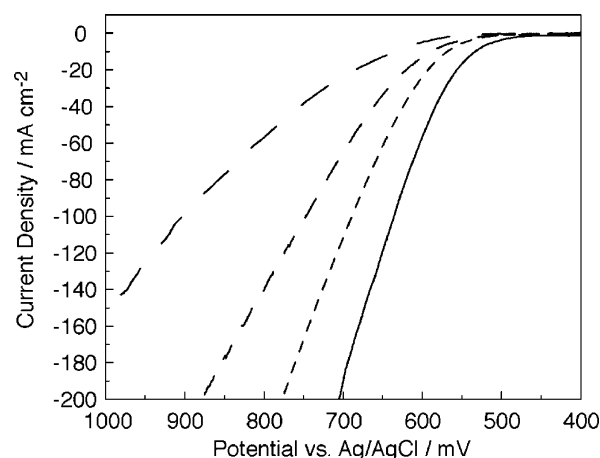

Figure 2. Size-dependent polarization activities for Ni foam working electrodes loaded with Co_3O_4 nanoparticles swept from 200 to 1000 mV (400−1000 shown) vs Ag/AgCl at 1 mV/s in 1.0 M KOH (pH 14): 5.9 (—), 21.1 (- - -), 46.9 nm (− − −), and bare Ni foam (− − −). All potentials are recorded using 1 cm² Ni foam working electrodes with catalyst loadings of 1 mg/cm².

TABLE 2: Electrochemical Characteristics Observed for the Co_3O_4 Nanoparticle Anodes

	potential at specified current density (mV)			
size (nm)	10 mA/cm²	50 mA/cm²	100 mA/cm²	200 mA/cm²
5.9	534	594	636	706
21.1	569	637	689	777
46.9	588	678	748	880
bare Ni	634	782	903	NA

reactions 3−5 represent a plausible sequence, there is little consensus in the literature as to the details of this process.[8]

The gaseous products were identified in a separate experiment using a single-compartment airtight electrochemical cell attached to a high-vacuum line and an in-line mass spectrometer. Mass spectra of gas samples from the headspace above a 1.0 M KOH solution biased at 800 mV vs Ag/AgCl, using a 1 cm² Ni foam working electrode loaded with 1 mg of 5.9 nm Co_3O_4 particles, showed large signals at m/z values of 2 and 32, confirming the electrolysis of water to hydrogen and oxygen, respectively (Figures S2 and S3, Supporting Information). The provenance of the gaseous products was confirmed by [18]O labeling experiments. Thus, biasing the working electrode in ^{18}O-enriched alkaline solutions (8.45 mol % [18]O, based on H_2O + KOH) at 800 mV produced oxygen signals at m/z values of 32, 34, and 36 for $^{16,16}O_2$, $^{16,18}O_2$, and $^{18,18}O_2$, respectively (Figures S4 and S5, Supporting Information). The integrated intensity for the $^{32}O_2$ and $^{34}O_2$ signals gave a ratio of $^{32}O_2/^{34}O_2$ of 5.73, which compares well with the ratio of 5.41 predicted by a statistical distribution of the [18]O label into the evolved oxygen. The larger-than-predicted $^{32}O_2/^{34}O_2$ ratio could be due to a small leak of ambient air into the cell over the course of the bulk electrolysis experiment but could also stem from the previously observed incorporation of lattice oxygen atoms contained in the cobalt oxide into the evolved oxygen observed for related $NiCo_2O_4$ anodes.[21,22]

The Co_3O_4 anodes are highly active electrocatalysts for oxygen evolution in alkaline solution. Scanning the anode potential from 200 to 1000 mV (vs Ag/AgCl, not corrected for Ohmic losses) at 1 mV/s in 1 M KOH produced a large current response that was markedly dependent on nanoparticle size (Figure 2). The maximal activity was observed for the anode loaded with 1 mg/cm² of small Co_3O_4 nanoparticles, which

Size-Dependent Activity of Co$_3$O$_4$ Nanoparticle Anodes

J. Phys. Chem. C, Vol. 113, No. 33, 2009 **15071**

TABLE 3: Selected Characterization and Electrocatalytic Activity Data for Co$_3$O$_4$ Anodes Examined under Conditions Similar to This Report

entry	BET SA (m^2 g^{-1})	loading (mg cm^{-2})	j (mA cm^{-2})	η (mV)	TOF × 10^3 (s^{-1})[a]	TOF* × 10^6 (s^{-1} m^{-2})[b]	TOF (s^{-1} Co$_{surf}$$^{-1}$)[c]	ref
1[d]	8	~7.5	10	410	2.49	0.43	NA	12
2	NA	~2.4	10	475	7.8	NA	NA	13
3	18.9	~3.4	50	199	27.6	1.2	NA	14
4	111.2	1	10	328	18.7	0.23	0.024	e
5	111.2	1	50	388	93.0	2.0	0.12	e

[a] Turnover frequency calculations for oxygen evolution calculated in mols of O$_2$ assuming that every cobalt atom is catalytically active (lower bound). [b] Turnover frequency calculations for oxygen evolution calculated in mols of O$_2$ assuming that every m^2 of Co$_3$O$_4$ surface area is catalytically active (upper bound). [c] Turnover frequency calculations for oxygen evolution calculated in molecules of O$_2$ assuming that every surface Co atom is active (see Supporting Information for details). [d] This study was conducted in 5 M KOH, pH 14.7 using a dynamic hydrogen reference electrode giving a thermodynamic potential for oxygen production of 166 mV vs Ag/AgCl. [e] This work.

achieved a current density of 10 mA/cm^2 at 534 mV (an overpotential of 328 mV). The larger particles reached current densities of 10 mA/cm^2 at slightly more positive potentials of 569 and 588 mV, respectively. Under the conditions of this study current densities of 200 mA/cm^2 could be achieved, albeit at significant, though not unreasonably high, anodic overpotentials (Table 2).

Direct comparison of electrocatalytic activities for different preparations of Co$_3$O$_4$ reported in the literature is difficult. Many factors affect the observed current densities, including the method of catalyst preparation, catalyst loading, substrate (Ni or Ti foils or meshes are most common), hydroxide concentration (1−8 M KOH in most reports), anode potential, solution temperature (the thermodynamic potential for water splitting decreases with increasing temperature), and pressure. A small sample of catalytic studies conducted under conditions similar to those used in this report is presented in Table 3.

The nanoparticle electrodes prepared in this report are more active than those reported by Rasiyah and Tseung[12] and Iwakara et al.,[13] achieving current densities of 10 mA/cm^2 at overpotentials that are between 80 and 140 mV less positive. Moreover, the catalyst loading required to achieve this current density is significantly lower by a factor of ~2.5−7 (comparing entries 1, 2, and 4). Using this data, turnover frequencies (TOFs) for oxygen evolution can be calculated on a per-molar basis, assuming 100% Faradaic efficiency and that every cobalt atom is catalytically active (effectively a lower bound on activity). Carrying through with this calculation, the nanoparticles reported here achieve a TOF of 1.87 × 10^{-2} s^{-1}. Alternatively, computing TOF on the basis of surface area, again assuming 100% Faradaic efficiency and that every m^2 of surface is catalytically active (an upper bound on activity) gives for entry 4 a TOF of 0.23 × 10^6 s^{-1} m^{-2} Co$_3$O$_4$, which is approximately half that of entry 1. In summary, for entries 1, 2, and 4 it is observed that at a fixed current density (i.e., reaction rate) an increase in catalyst surface area increases the activity on a per-mole basis and consequently decreases the driving force (overpotential) required to maintain that reaction rate. The microwave-synthesized Co$_3$O$_4$ reported by Singh and co-workers[14] in entry 3 is reported to be active at lower electrochemical overpotentials than the much higher surface area nanoparticles considered here. Comparing entries 3 and 5 it is observed that the overpotential to achieve a current density of 50 mA/cm^2 is reported to be ~190 mV lower than that for the materials prepared for this study. While the reported activity of the Co$_3$O$_4$ anodes reported by Singh appears impressive, experimental complications may be responsible for the unusually high current density. Singh and coworkers conduct their electrocatalytic measurements in a single compartment electrochemical cell. This means that the reaction products generated at the cathode are not segregated from the
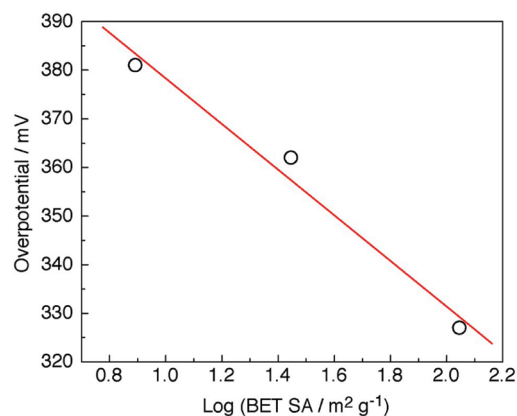

Figure 3. Plot of the electrochemical overpotential for water oxidation at a constant current density of 10 mA/cm^2 against the log of the BET surface area for the isolated Co$_3$O$_4$ nanoparticles. The linear regression shows a line of slope −47 ± 7 mV/dec.

anode. In this case the hydrogen produced at the cathode can readily be reoxidized at the anode (already poised at ~1.5 V overpotential for H$_2$ oxidation). In a system such as this, large spurious currents are expected for the very facile oxidation of hydrogen, leading to inflated anodic current densities and less than unity Faradaic efficiencies.[23]

The effects of nanoparticle surface area on the anode activity were determined using the Tafel equation, eq 4, where i is the observed current, i_o is the exchange current, S is the surface area, L is the catalyst loading, η is the overpotential, and b is the Tafel slope.

$$i = i_o SL \exp(\eta/b) \quad (4)$$

Figure 2 shows that within the Tafel region ($i = 10$ mA/cm^2, see Supporting Information, Figure S6) one can find a region where i, i_o, L, and b are constant. For this region eq 4 can be rearranged to give eq 5.

$$\eta = \text{constant} - b \log S \quad (5)$$

Wherein a semilog plot of the polarization data for the small, medium, and large Co$_3$O$_4$ nanoparticle loaded anodes against the logarithm of the BET surface area of the isolated nanoparticles gives a linear relation with a slope of $b = -47 \pm 7$ mV/dec, Figure 3. This correlation suggests that with all other factors constant, an increase in the catalyst surface area by an order of magnitude will decrease the overpotential (for a given current density) by ~ 50 mV.

Conclusions

In conclusion, this report has shown that cubic nanoparticles of Co_3O_4 are active anode materials for water oxidation in alkaline solution. Significantly, the precision of nanoparticle synthesis allows for the effects of catalyst surface area to be determined from the polarization data in a well-defined way. As this work has shown, for Co_3O_4 anodes, an increase in the catalyst surface area by an order of magnitude decreases the overpotential required to achieve a specific current density by ~50 mV. Future work will explore the shape dependence of Co_3O_4 nanoparticles to determine whether various crystal faces are more or less active for oxygen evolution.

Supporting Information Available: Cyclic voltammograms of the bare and loaded electrodes, mass spectrographs of the gaseous products, Tafel representations of the polarization data, and details of the TOF per surface cobalt calculations. This material is available free of charge via the Internet at http://pubs.acs.org.

References and Notes

(1) Hoffert, M. I.; Caldeira, K.; Jain, A. K.; Haites, E. F.; Harvey, D. L. D.; Potter, S. D.; Schlesinger, M. E.; Schneider, S. H.; Watts, R. G.; Wigley, T. M. L.; Wuebbles, D. J. *Nature* **1998**, *395*, 881.

(2) Lewis, N. S.; Nocera, D. G. *Proc. Nat. Acad. Sci.* **2006**, *103*, 15729.

(3) Kanan, M. W.; Surendranath, Y.; Nocera, D. G. *Chem. Soc. Rev.* **2009**, *38*, 109.

(4) Trasatti, S. *Int. J. Hydrogen Energy* **1995**, *20*, 835.

(5) Tarasevich, M. R.; Efremov, B. N. *Electrodes of Conductive Metal Oxides*; Trasatti, S., Ed.; Elsevier: Amsterdam, 1980; Chapter 5, and references therein.

(6) Jiao, F.; Frei, H. *Angew. Chem., Int. Ed.* **2009**, *48*, 1841.

(7) Trasatti, S. *Transition Metal Oxides: Versatile Materials for Electrocatalysis*; Lipkowski, J., Ross, P. N., Eds.; Electrochemistry of Novel Materials, VCH Publishers Inc.: New York, 1994, and references therein.

(8) Matsumoto, Y.; Sato, E. *Mater. Chem. Phys.* **1986**, *14*, 397, and references therein.

(9) Boggio, R.; Carugati, A.; Lodi, G.; Trasatti, S. *J. Appl. Electrochem.* **1985**, *15*, 335.

(10) Marbán, G.; López, I.; Valdéz-Solís, T.; Fuertez, A. B. *Int. J. Hydrogen Energy* **2008**, *33*, 6687.

(11) Cox, P.; Pletcher, D. *J. Appl. Electrochem.* **1990**, *20*, 549.

(12) Rasiyah, P.; Tseung, A. C. C. *J. Electrochem. Soc.* **1983**, 365.

(13) Iwakara, C.; Honji, A.; Tamura, H. *Electrochim. Acta* **1981**, *26*, 1319.

(14) Singh, R. N.; Mishra, D.; Anindita, Sinha, A. S. K.; Singh, A. *Electrochem. Commun.* **2007**, *9*, 1369.

(15) Jiang, S. P.; Lin, Z. G.; Tseung, A. C. C. *J. Electrochem. Soc.* **1990**, *137*, 764.

(16) Li, Y.; Tan, B.; Wu, Y. *Nano Lett.* **2008**, *8*, 265.

(17) Kanan, M. W.; Nocera, D. G. *Science* **2008**, *321*, 1072.

(18) Dong, Y.; He, K.; Yin, L.; Zhang, A. *Nanotechnology* **2007**, *18*, 435602.

(19) Guinier, A. *X-ray Diffraction*; W. H. Freeman: San Francisco, 1963.

(20) Trasatti, S. In *Electrochemical Hydrogen Technologies*; Wendt, H., Ed.; Elsevier: Amsterdam, 1990; p 104.

(21) Hibbert, D. B.; Churchill, C. R. *J. Chem. Soc., Faraday Trans. I* **1984**, *80*, 1965.

(22) Hibbert, D. B. *J. Chem. Soc., Chem. Commun.* **1980**, 202.

(23) This phenomenon is necessarily system dependent (anode/cathode separation, cell volume, etc.) and cannot easily be corrected for after the fact.